Pol. J. Environ. Stud. Vol. 32, No. 3 (2023), 2281-2291
DOI: *10.15244/pjoes/157495* ONLINE PUBLICATION DATE: 2023-02-23

Original Research

Impact of Land Cover Changing on Wetland Surface Temperature Based on Multitemporal Remote Sensing Data

Nurlina[1,4]*, Syarifuddin Kadir[2], Ahmad Kurnain[3], Wahyuni Ilham[2], Ichsan Ridwan[4]

[1]Doctoral Program of Agriculture Science, Postgraduate Lambung Mangkurat University, Banjarbaru, South Kalimantan, Indonesia
[2]Faculty of Forestry, Lambung Mangkurat University, Banjarbaru 70714, South Kalimantan, Indonesia
[3]Faculty of Agriculture, Lambung Mangkurat University, Banjarbaru 70714, South Kalimantan, Indonesia
[4] Faculty of Mathematical and Natural Science, Lambung Mangkurat University, Banjarbaru 70714, South Kalimantan, Indonesia

Received: 10 September 2022
Accepted: 14 December 2022

Abstract

Changes in land use and land cover (LULC) have been studied in recent years. Urban/rural planning, temperature analysis, and environmental monitoring can benefit from examining these variations. Land surface temperature (LST) has a great potential to act as a global indicator of the status of wetlands and changes in their hydrological and evapotranspiration regimes, which are often linked to land use and cover changes. Using remote sensing data, several studies have examined LULC changes on LST. This multi-temporal analysis used images from Landsat during 2005 to 2020. This study compares surface biophysical properties to sub-pixel heat changes. This result shows that LULC classes have different LST. Expansion of Oil Palm plantations decreases LST, while bare land and impervious surface increases it. The LST declined 3ºC (0.115ºC each year) over 20 years in the research area. This research provides information demonstrating how plantation growth from deforestation raises the surface temperature. Meanwhile, plantation from shrub and bareland decrease the surface temperature. The development of LST trend maps and time series charts on an operational basis give wetland managers with a fast and dependable single indicator of the effect of land processes on water and energy flows, allowing them to better managing their wetlands. Continuous monitoring of LULC dynamics is needed to design sustainable land use regulations for environmental preservation and regional economic development.

Keywords: land surface temperature, land use/land cover, emissivity, NDVI, Tabunio watershed

*e-mail: nurlina_abdullah@ulm.ac.id

Introduction

In addition to offering a wide range of functions, wetland habitats have numerous values [1]. In some circumstances, wetlands provide the only source of natural resources available to rural communities, allowing them to survive and thrive. Their plant communities contain a vast range of vegetation types, densities, and water demands and availability, among other characteristics. It is difficult to predict wetland environment such as their water requirements and consequences on streamflows, and agricultural activities have a significant impact on their operation. Remote sensing imaging has been frequently employed for monitoring wetlands because it can offer information on their environmental status that is both regionally spread and temporally frequent [1-3].

Most monitoring systems employ LULC change techniques or optical [4] or radar time series to map water surface dynamics [5]. Thermal infrared data is rarely used, yet it can help understand evapotranspiration in groundwater-dependent ecosystems. LST-based evapotranspiration estimations produced from thermal data are useful in water management and water rights issues [1, 6]. Using LST fluctuations, it may be feasible to detect changes in land management methods without a direct change in land cover types [7] and to map wetlands beneath aquatic vegetation [8]. LST reacts to drought earlier than NDVI, which is a benefit [9]. When working with LST data, one of the most challenging aspects is the considerable temporal variability of the data; it is highly dependent on meteorological and lighting circumstances, and assessing the change in LST between two single points in time is ecologically insignificant [10]. Landscape change patterns impacting water balances and energy fluxes can be revealed through the analysis of dense LST time series. Especially essential in highly dynamic and water-dependent ecosystems such as wetlands is the concept of resiliency. While having a coarse resolution (1 km), the daily MODIS LST products are appropriate for time series analysis due to the fact that they have been providing daily LST data at a global level since 2000 [11].

In addition to the noise caused by atmospheric effects, distinguishing between seasonal correlations, gradual correlations, and abrupt correlations, all of which are combined in time series data [7, 12], is a second challenge that must be overcome when analyzing LST time series. This challenge was previously mentioned. Temporal series analysis can be carried out through the extraction of data and its subsequent aggregation into statistical parameters [13], through the application of harmonic analysis [7], or by utilizing change detection algorithms and unsupervised classification of the changes [7, 14]. In order to address these issues, methods such as Breaks For Additive Seasonal and Trend (BFAST) [15], and greenbrown [16, 17] have been developed. They examine data by breaking it down into three components: seasonal fluctuation, trend, and a residual portion of the data [18]. Break spots resulting from abrupt changes in the land cover attributes are identified and marked.

Unpredictable time steps generated by gaps owing to clouds and other phenomena provide a third problem, which results in low pixel quality, which is labeled as such in the quality band. It has been intended to analyze trends, trend changes, and phenology events in gridded time series of vegetation indexes while interpolating missing data. The open source R package greenbrown is available for download here. Both of these indicators of vegetation cover and health condition are commonly employed in time series analysis to examine the changes in vegetation cover and health status [19]. However, because the surface water dynamics of some wetlands are very changeable, vegetation indices are less suitable for determining long-term trends in these ecosystems. NDVI decreases can occur as a result of a loss of vegetation or as a result of an increase in floods, among other reasons. LST will rise as a result of both losses in plant cover and increases in water content, on the other hand, and vice versa. Despite this, we uncover fewer examples of the use of LST to monitor long-term changes than we would have expected. Whenever LST is used for monitoring, it is frequently combined with NDVI [9, 20] or is primarily concerned with climatology [16, 20]. Additionally, the link between NDVI and LST has been investigated earlier; when energy is the limiting factor, NDVI and LST have a positive association, but when water is the limiting factor, LST and NDVI have a negative correlation [21]. With all these advantages, LST can be fully utilized to evaluate temporal patterns in water-based ecosystems, to the best of our knowledge. The purpose of this project is to evaluate the potential of land surface temperature (LST) as an indication of land use change in the Tabunio watershed, which will serve as a study region. There has been significant land conversion to Plantation in the Tabunio watershed over the last two decades, and the consequences of these conversions are still not fully understood. The Tabunio watershed is a large complex of wetlands that has seen significant land conversion to plantation over the last two decades. With the use of the whole Landsat archive (2005-2020) of LST and NDVI products, as well as a set of Landsat-based LULC change maps, the spatio-temporal changes of LST and NDVI in Tabunio watershed were investigated and appraised in relation to these land conversions in Tabunio watershed.

Material and Methods

Study Area

The environmental damage that occurs in the Tabunio watershed needs serious attention, the increasing area of critical land, the high level of erosion,

and the decreasing water catchment area have resulted in floods and droughts from year to year. For this reason, research is needed to anticipate this and identify areas that are vulnerable to environmental damage in the Tabunio watershed.

Tabunio watershed, which is located in Tanah Laut Regency and has an area of 62,558.56 ha and is physically located at 3°37'2.72"-3°51' 51.43" South Latitude and 114°36' 12.02"-114°57'47.62" East Longitude, is where the research is being conducted. Administratively, the Tabunio watershed includes a total of 44 communities, as well as 4 sub-districts and 10 sub-watersheds (ecologically). Fig. 1 is a map that displays the location of the research being conducted for the Tabunio watershed.

The decision was made to use satellite images as the primary source of data for this investigation because of its high resolution, ability to account for atmospheric conditions, consistency, and rapid update rates. In order to generate LULC and LST maps, the United States Geological Survey (USGS) Earth Explorer in 2020, uses three cloud-free Landsat Level 2 images from 2005 (Landsat 5 TM), 2010 (Landsat 5 TM), 2015 (Landsat 8 OLI/TIRS), and 2020 (Landsat 8 OLI/TIRS). These images were acquired between 2005 and 2020. All of the Landsat images have a spatial resolution of 30 meters and were captured within the same month so as to eliminate the influence of temperature. Surface reflectance is the unit of measurement used for the multispectral bands acquired by Landsat 5 TM and Landsat 8 OLI/TIRS. Radiance and a digital integer are transformed into reflectance values to determine surface reflectance.

NDVI is founded on the premise that healthy vegetation visibly reflects in the near-infrared section of the electromagnetic spectrum, with green leaves reflecting 20% or less in the 0.5 to 0.7 m range (green to red) and 60% in the 0.7 to 1.3 m range (near-infrared). Sobrino et al. (2004) based the vegetative index on the expression.

$$NDVI = \frac{NIR-Red}{NIR+Red} \tag{1}$$

In order to classify the surface emissivity for the various land covers that were considered, emissivity correction was utilized. In order to calculate the final LST, the surface emissivity calculated based on NDVI classes was applied [7].

$$\varepsilon_{TM6} = 0.004P_v + 0.986 \tag{2}$$

where ε and P_v represent land surface emissivity and the proportion of vegetation acquired. However, P_v can be calculated using Sobrino et al. (2004):

$$P_v = \left[\frac{NDVI-NDVI_{min}}{NDVI_{max}-NDVI_{min}}\right]^2 \tag{3}$$

LST is obtained from data collected by LandsatTM. LST is derived from data collected by LandsatTM. The values of the LST are determined by following a method that consists of three steps. First, the picture pixels that make up the digital numbers are converted to surface radiance by utilizing sensor-specific calibration standard values. In the second step, the radiance values are converted to an equivalent temperature range for dark bodies. In the third phase, the emissivity-corrected temperature and the type of land cover that is relevant to the calculation are both determined. The approach that was just described was carried out on both of the sensors. Using the TIR band 6 on Landsat-5 TM, a calculation was made to determine the surface temperature of the region.

The transformation from digital numbers, to radiance LTM.

$$\text{LTM} = 0.124+0.00563*\text{DN} \tag{4}$$

The radiance to equivalent blackbody temperature TTMSurface at the satellite using

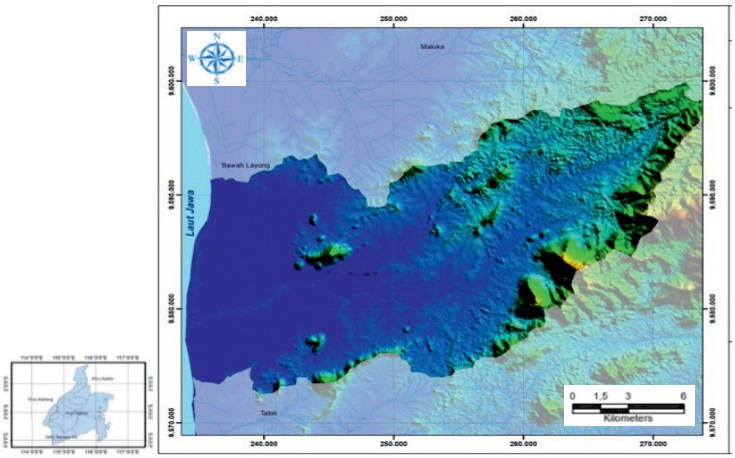

Fig. 1. Research location Map of Tabunio Watershed.

$$TTMSurface = [K2 /(K1-lnLTM)] -273 \quad (5)$$

For Landsat TM, K1 = 4.127 and K2 = 1274, respectively, the coefficients K1 and K2 are dependent on the range of blackbody temperatures.

To account for the non-uniform emissivity of the land surface, an extra correction for spectral emissivity (ε) is required. Emissivity correction is carried out using surface emissivities for the specified LC (Table 1) derived from the methodology described in [22]. The emissivity corrected land surface temperature (Ts) was finally computed as follows [7].

$$T_S = \frac{T_B}{1+\left(\lambda x \frac{T_B}{\rho}\right) \ln \epsilon} \quad (6)$$

where, λ is the wavelength of emitted radiance for which the peak response and the average of the limiting wavelengths (λ = 11.5 µm) were used, ρ = h × c/σ (1.438 × 10-2 mK), σ = Stefan Boltzmann's constant (5.67 × 10-8 Wm-2 K-4 = 1.38 × 10-23 J/K), h = Planck's constant (6.626 × 10-34 Jsec), c = velocity of light (2.998 × 108 m/sec), and ε is spectral emissivity (Table 1).

LST from Landsat ETM+

The procedure follows same principle as done for Tm data. The TIR image Landsat ETM+ of (band 6) DN was first converted into spectral radiance L_{ETM} using Equation (5), and then converted to equivalent black body temperature,$T_{ETM\ Surface}$, under the assumption of uniform emissivity (ε ≈ 1) using Equation (6) [23].

$$L_{ETM} = 0.0370588*DN+3.2 \quad (7)$$

$$T_{ETMsurface} = \left[\frac{K2}{ln\left(\frac{K1}{L_{ETM}}+1\right)}\right] \quad (8)$$

Where, $T_{ETMSurface}$ is effective at satellite temperature in Kelvin, L_{ETM} is spectral radiance in watts/(meters squared×ster×µm). For Landsat-7 ETM+, K2 = 1282.71 K and K1 = 666.09 $mWcm^{-2}$ sr^{-1} μm^{-1} were used. The emissivity corrected land surface temperatures Ts were finally computed by Equation (6). During the process, the NDVI was computed by making use of the bands Red and NIR, and the NDVI output image was then utilized in order to compute the emissivity. When estimating LST, the normalized difference vegetation index (NDVI) is utilized since the amount of vegetation that is currently present is a crucial component, and the NDVI may be used to simulate general vegetation conditions (Weng et al. 2004).

Results and Discussion

Land Use/Land Cover Change

Land use/cover factors are derived from Landsat image data that have been categorised using the ROI (Region of Interest) as a reference point. For each year of research, there are two types of ROI samples: training samples and testing samples. The training sample is used as a representative sample for land cover classification, whereas the testing sample is used as a representative sample for land cover classification with reference to Google Earth, which will subsequently be used to assess the classification's accuracy. The number of ROI samples varies by more than 100 pixels for each land cover. Water bodies, marshes, ponds, mines, bushes, agriculture, forests, plantations, settlements, and barren terrain are all categorised as different types of land cover. The Support Vector Machine Classification approach was chosen due to its ability to produce the most representative findings. Additionally, the confusion matrix and Kappa coefficients are used to generate and verify overall accuracy (OA), user accuracy (UA), and

Table 1. Land Use/Land Cover Data in Tabunio Watershed 2005-2020.

Land Use/Land Cover	Tahun			
	2005 (acres)	2010 (acres)	2015 (acres)	2020 (acres)
Water body	592,64	386,64	368,50	406,48
Forest	16.223,67	14.004,85	14.699,89	13.166,88
Bare land	3.712,99	4.945,80	13.247,55	7.906,35
Residential	619,07	991,83	1.451,73	2.001,24
Plantation	502,16	7.710,81	20.866,44	24.313,31
Agriculture	21.021,27	10.313,42	8.366,95	12.917,27
Swamp	6.759,52	3.818,56	161,37	181,88
Shrubs	10.846,53	17.042,34	1.695,94	1.216,33
Pond	45,88	126,24	47,96	36,14
Mining	2.172,66	3.155,88	1.590,04	350,50

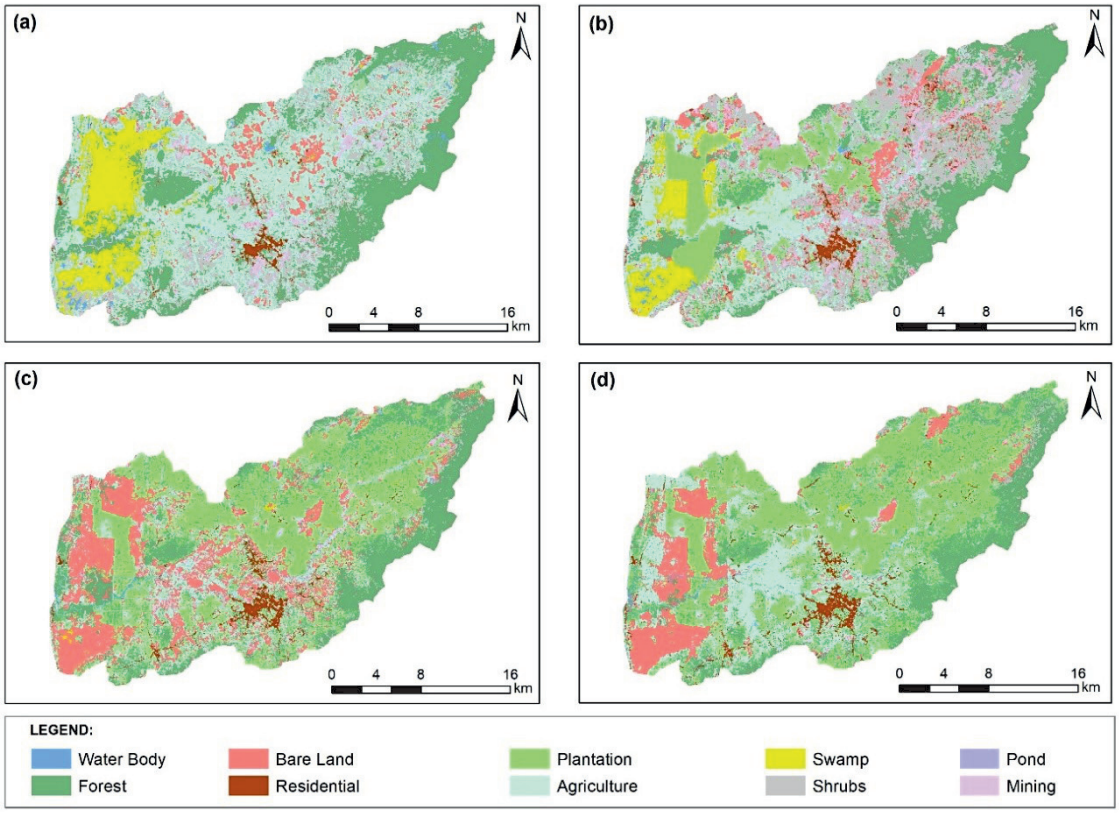

Fig. 2. Land use/land cover Map of Tabunio Watershed a) 2005 b) 2010 c) 2015 and d) 2020.

producer accuracy (PA). All categorization findings demonstrate a high overall accuracy (OA) of between 86 and 95 percent (Nurlina et al. 2021).

Significant changes include an increase in residential and plantations, as well as a significant reduction in forest and shrub cover. Residential coverage increased by 1,382.17 hectares (from 619,07 hectares in 2005 to 2.001,24 hectares in 2020), a 323.26 percent increase, while plantations increased by 23,811.15 hectares (from 502,16 hectares in 2005 to 24,313.31hectares in 2020), a 4,841.7 percent increase, while forests decreased by 3,056.79 hectares (from 16.223,67 to 13,166.88 hectares in 2020), a 81.5 percent. Figs 4(a-d), Table 1 and Table 2 illustrate the historical changes in land cover in the research area from 2005 to 2020 [24]. The continuous clearing of riverbank vegetation covers typically contributes to the instability of riverbanks and, as a result, an accompanying expansion in bank width. It's possible that this is one of the primary contributors to the expansion of the total land area covered by water bodies. In light of the information presented above, it is abundantly clear that the rapid rate of urbanization

Table 2. Table of Land Cover Changes in the Tabunio Watershed 2005-2020.

Land Cover	Area of Change			
	2005-2010 (acre)	2010-2015 (acre)	2015-2020 (acre)	2005-2020 (acre)
Water body	-206,00	-18,14	37,98	-186,16
Forest	-2.218,82	695,04	-1.533,01	-3.056,79
Bare land	1.232,82	8.301,75	-5.341,20	4.193,36
Residential	372,77	459,90	549,51	1.382,18
Plantation	7.208,65	13.155,63	3.446,87	23.811,15
Agriculture	-10.707,86	-1.946,46	4.550,32	-8.104,00
Swamp	-2.940,96	-3.657,19	20,50	-6.577,65
Shrubs	6.195,82	-15.346,40	-479,62	-9.630,20
Pond	80,37	-78,28	-11,82	-9,73
Mining	983,22	-1.565,85	-1.239,54	-1.822,17

and the urban sprawl situation that is associated with it are clearly reflected in the land use/land cover changes that will occur over the watershed between the years 2005 and 2020 as analyzed in this study (Fig. 2). As a result, this has a significant impact on the ecosystem and the microclimate of the watershed, which can be seen reflected in the pattern of the temperature of the land surface [25].

NDVI/Emissivity

The normalized difference vegetation index (NDVI) is a measure of vegetation intensity that allows for the differentiation of various plant types and non-vegetated surfaces. In 2005, the vegetative cover in the watershed's center was significantly reduced, resulting in a low NDVI value of roughly 0.3. (Fig. 3). This NDVI value often increases as one moves away from the city's centre toward its periphery, indicating a response to diminishing land use intensity. Areas with a moderate to low build up density had an NDVI value of -0.5, whereas water bodies and forest had a higher NDVI value of about 0.77. By 2005, significant changes had occurred, as the spatial breadth of green areas had been substantially reduced as a result of growing urbanization throughout the city (Fig. 2). The spatial expanse of vegetative land cover in 2020 has decreased significantly from 2005. The NDVI was used to estimate the emissivity values for the various land use types, and the estimation threshold is shown in Table 3. For 2005, 2010, 2015, and 2020, the emissivity value is between 0.955 and 0.985 in the central business district and 0.985 in the periphery business district: built-up regions have higher emissivity values, while water bodies and vegetation have lower emissivity values (Fig. 3 and Fig. 4). Variations in the Normalized Difference Vegetation Index (NDVI) reflect the global land surface vegetation coverage, which is important for the analysis of the ecological environment [26].

Table 3. Land surface temperature variation (ºC) in Tabunio Watershed from 2005 to 2020.

Year	Min (ºC)	Max (ºC)
2005	16	31
2010	14	29
2015	12	28
2020	17	28

Land Surface Temperature

The regional distribution of land surface temperature in 2005 revealed a range of values between 16 and 31 degrees Celsius, with the bareland and shrubs having the greatest value (Fig. 5a). The lowest LST value of 16ºC was attributed to water bodies and forest. The mean temperature was 25.3 degrees Celsius. However, for 2010, the regional distribution of land surface temperature is between 14 and 29 degrees Celsius (Fig. 5b). In 2015, when the LST value spans

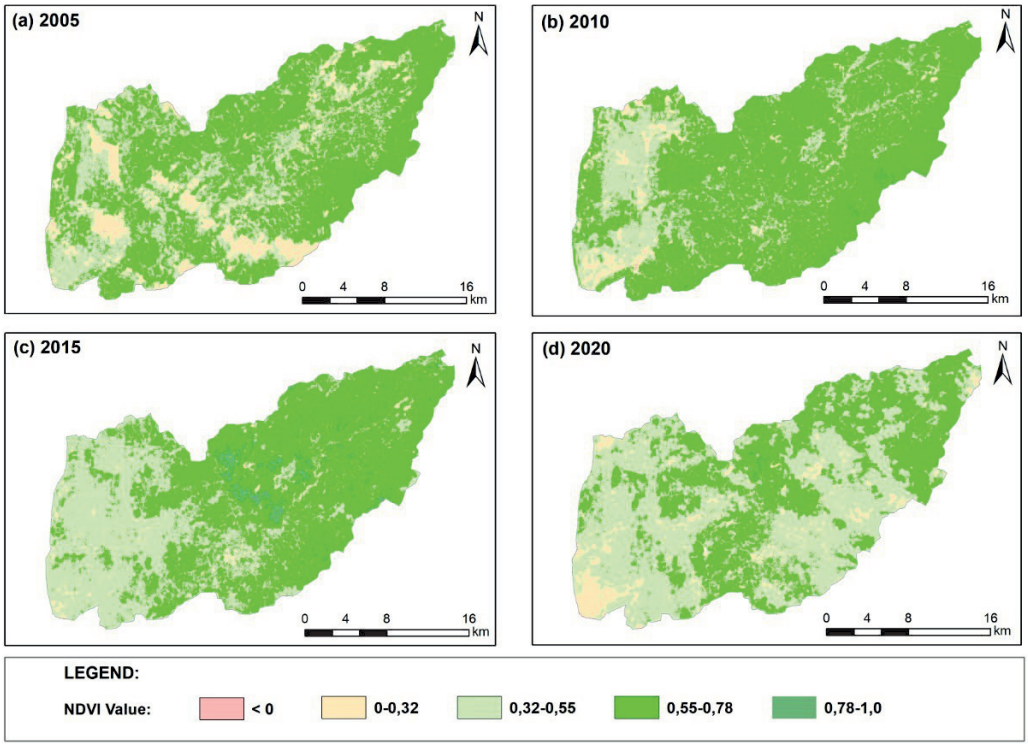

Fig. 3. NDVI map of Tabunio Watershed 2005-2020 a) 2005 b) 2010 c) 2015 and d) 2020.

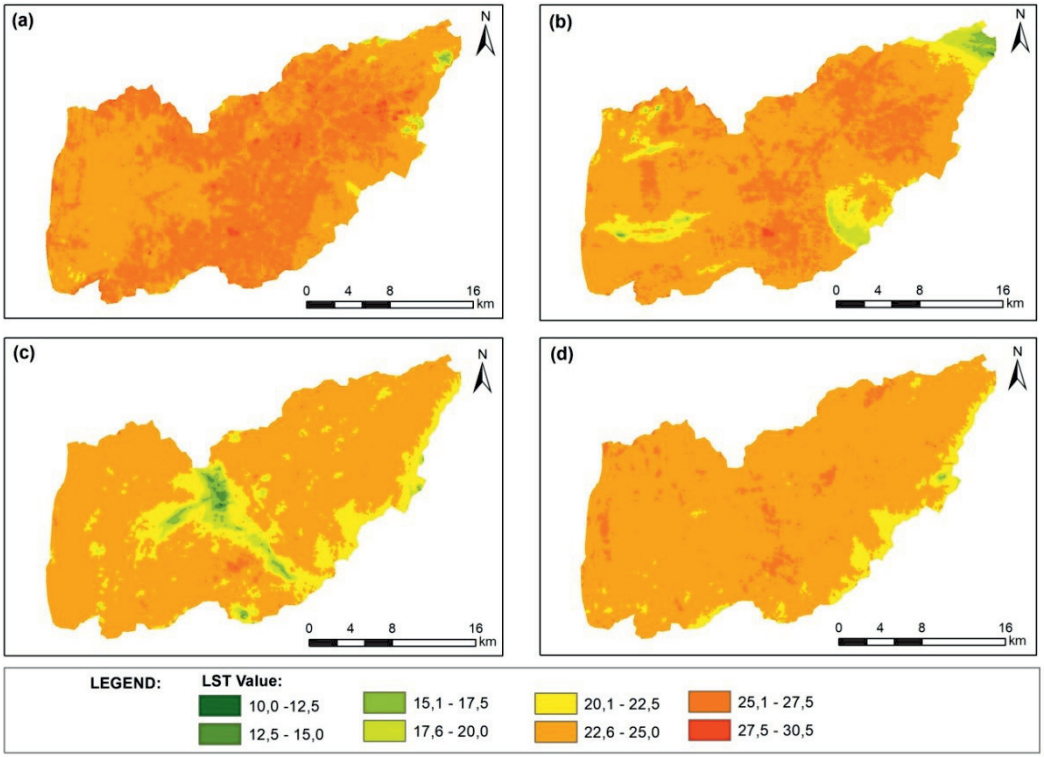

Fig. 4. Land surface temperature of Tabunio Watershed a) 2005 b) 2010 c) 2015 and d) 2020.

between 12 and 28 degrees Celsius, a dramatic increase was seen (Fig. 5c). For 2020, the regional distribution of land surface temperature is between 17 and 28 degrees Celsius (Fig. 5d). The LST values varied significantly across the city's various land use/land cover classifications. The temperature of the built-up area decresed by -1.61ºC, the bareland by -3.38ºC, and the vegetation by -1.48ºC, whereas the temperature of the water bodies decreased by -2.7ºC. It was importantly noted that the growth of plantation areas, reduced shrubs and bareland cover resulted decreased in the study area's LST. Reduced forest area resulted an increased in temperature in the surrounding area. This implies that a causal relationship exists between land cover dynamics and patterns of LST occurrence across the study area. Additionally, a 300 percent change in plantation resulted in a 1.1 percent temperature decreased. Additionally, a 21 percent loss in vegetative cover from natural heavy canopies to almost grassland in 2005 led in a 15.2 percent increase in temperature. In 2020, exposed surfaces grew by 212 percent in the research area, implying a 5.8 percent temperature increase.

Disturbances such as deforestation induce a break in the time series, drastically boosting the LST. As vegetation begins to regenerate in the years following deforestation, it would be predicted that LST would exhibit a decreasing trend (Table 3). The decline in the value of LST was also due to the fact that 2005 was the warmest year in over a century, according to NASA scientists studying temperature data from around the world (https://www.nasa.gov/vision/earth/environment/2005_ warmest.html), while from the trend of the data, LST has increased again in 2020, this is in accordance with the statement from Scientists from Copernicus that also have 2020 as the warmest year on record, while the United Kingdom Met Office ranked 2020 as the second-warmest year on record (https://www.noaa.gov/news/2020-was-earth-s-2nd-hottest-year-just-behind-2016). In our case, expansion of plantations was also associated with decreased in LST due to reduced land cover from shrubs and bare land to oil palm plantations. However, when natural vegetation (forest or wetland) is replaced by plantation, LST trends to continue increasing. The expansion of oil palm plantations and other cash crops results in changes in biophysical variables, which warms the land surface and so contributes to the increase in air temperature caused by climate change, as well as the warming of the land surface [27, 28].

The area's rapid population growth, combined with a lack of property rights, has resulted in unregulated plantation development and deforestation [10, 29, 30]. The majority of the increases in LST and plantation expansion patterns occurred within the Tabunio watershed, which contain numerous natural resources (mainly water, wood, and fertile lands). Areas of permanent marshes and to the east of Tabunio watershed did not show significant increases in LST (nor decreases in NDVI). The periodically inundated grasslands at the heart of the Tabunio watershed site have remained largely uninhabited, owing to the fact that

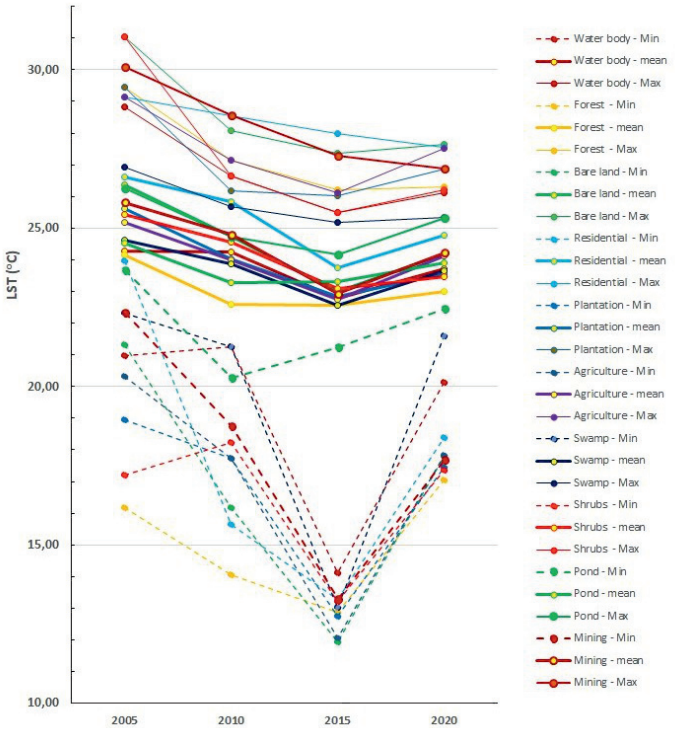

Fig. 5. Graphic of land surface temperature with landuse/landcover type Tabunio Watershed in 2005-2020.

plantation expansion is constrained by recurrent floods. They do, however, exhibit modest increases in LST (but not in NDVI), Implying that oil palm operations may be altering the water balance in these seasonally flooded areas. This is consistent with the findings of [1, 27], who determined that land cover changes reduce evapotranspiration and baseflow while boosting runoff. Climate change processes may also have an effect on the floodplain's evapotransporation regimes, although 20 years is insufficient time to draw such conclusions.

Errors are unavoidable when converting continuous patterns on the land surface to discrete classes. The Forestation class was overstated in our situation (Table 4). As a result of this, and the considerable spatial resolution disparity between the LULC change map (30 m) and the LST data set, the overall changes in LST for the Forestation class were inconclusive. The LST, on the other hand, reduced significantly in locations where ground truth data indicated genuine forestation of grasslands (Fig. 5d). The results were more straightforward for the other types of land change: LST increased in regions of residential and

Table 4. LST value in different land use/land cover.

Land use/land cover	Land Surface Temperature (ºC)							
	2005		2010		2015		2020	
	Min	Max	Min	Max	Min	Max	Min	Max
Water body	20.99	28.83	21.27	26.65	14.11	25.49	20.14	26.13
Forest	16.17	29.46	14.07	27.13	12.86	26.22	17.04	26.30
Bare land	21.32	31.03	16.17	28.08	11.93	27.36	17.81	27.65
Residential	23.98	29.15	15.65	28.55	13.27	27.99	18.39	27.54
Plantation	18.95	29.46	17.72	26.17	12.74	26.03	17.47	26.86
Agriculture	20.31	29.15	17.72	27.13	12.07	26.13	17.83	27.51
Swamp	22.33	26.91	21.27	25.69	13.02	25.19	21.59	25.34
Shrubs	17.22	31.03	18.24	26.65	13.22	25.50	17.37	26.21
Pond	23.66	26.27	20.27	24.72	21.23	24.18	22.46	25.33
Mining	22.33	30.09	18.75	28.55	13.30	27.28	17.69	26.87

mining expansion, while areas without LULC alterations also reported large increases in LST. It is worth noting that the Climate Change Initiative's newly issued yearly LULC reports continue to classify a major portion of the floodplain as flooded grasslands, despite the fact that it is widely utilized for agriculture and its ecological functions have been damaged [16, 20, 27]. The Ramsar Convention's notions of "Ecological Character" and "Wise Use" of wetlands suggest that wetland ecosystem services may be used to a certain extent, as long as the wetland system's integrity and health are not threatened [31]. Our findings, in conjunction with those of other researchers [27, 28, 31], suggest that plantation expansion may be eroding the wetland's ecological identity. Uncontrolled plantation usage of the wetland may even have an effect on places that remain largely natural, such as the centre of the floodplain (Fig. 5c). Land use/cover change has been confirmed to have a significant impact on climate through various aspects that modulate LST and precipitation [32, 33]. Forthcoming plans to modernize plantation in the area should take into account the water balance and the preservation of the ecosystem services provided by the wetland [34]. For example, updating farmers' energy sources could halt or significantly reduce deforestation caused by the use of lumber for fuel. The Tabunio floodplain's primary biological function was to act as a wildlife corridor of the Meratus Mountains National Park (Fig. 1). Restoring the Tabunio watershed would be a simple option in terms of connectivity. There are a few sites where LST has not increased, indicating that they are not yet substantially used by agriculture and may be subject to some form of protection. The evidence suggests that conservation regimes in the area have been somewhat successful in halting deforestation and farming development [35-38].

Conclusion

The land use/land cover analysis demonstrated changes in agricultural and forest lands and impermeable surfaces owing to urbanization. From 2005 to 2020, urban cover increased together with land surface temperature. Highly urbanized towns in Pelaihari have the greatest LST values, while the suburbs have low LST values. The study shows the ability of remote sensing and GIS for identifying land use land cover dynamics and land surface temperature.

The environmental consequences of plantation development and deforestation on wetlands are numerous and complicated in nature. However, certain impacts may not have an impact on the classification of a land cover, but they may have an impact on the biophysical variables of a land cover (productivity, spectral indices or LST). By analyzing LST dense time series, it is possible to determine the regional and temporal distribution of such impacts in wetlands. The quantitative information provided by these analyses can be particularly beneficial in vast areas experiencing rapid expansion and with limited access to field data, as they provide quantitative information in a timely way. Overall increases in LST corresponded to patterns of agriculture expansion and deforestation, and LST and NDVI were shown to be adversely associated. LST levels were found to be decreasing in both inhabited and unoccupied regions, where plantation and the number of cattle herders have both expanded dramatically in the previous decade, showing that their impact reaches into the still-natural areas as well.

The time period under consideration is far too short to take into account the effects of climate change. We do, however, give information demonstrating how plantation growth on wetlands raises the surface temperature, which in turn affects the temperature of the surrounding air and atmosphere. The development of LST trend maps and time series charts on an operational basis can give wetland managers with a quick and dependable single indicator of the effect of land processes on water and energy flows, allowing them to better manage their wetlands.

Acknowledgments

This research is financially supported by National Competitive Applied Research grant from the Ministry of Education, Culture, Research and Technology.

Conflict of Interest

All authors declare no conflicts of interest in this paper.

References

1. MURO J., STRAUCH A., HEINEMANN S., STEINBACH S., THONFELD F., WASKE B., DIEKKRÜGER B. Land surface temperature trends as indicator of land use changes in wetlands. International Journal of Applied Earth Observation and Geoinformation, **70** (February), 62, **2018**.
2. NURLINA, RIDWAN I., HADI HARYANTI N., HANIK U. Analysis of Environmental Vulnerability Using Satellite Imagery and Geographic Information System in Coal Mining Area Planning at Banjar Regency. IOP Conference Series: Earth and Environmental Science, **499**, 012014, **2020**.
3. MALEKMOHAMMADI B., JAHANISHAKIB F. Vulnerability assessment of wetland landscape ecosystem services using driver-pressure-state-impact-response (DPSIR) model. Ecological Indicators, **82** (March 2016), 293, **2017**.
4. YANG X., ZHAO S., QIN X., ZHAO N., LIANG L. Mapping of urban surface water bodies from sentinel-2 MSI imagery at 10 m resolution via NDWI-based image sharpening. Remote Sensing, **9** (6), 1, **2017**.
5. BUAKHAO W., KANGRANG A. DEM Resolution Impact on the Estimation of the Physical Characteristics

of Watersheds by Using SWAT. Advances in Civil Engineering, 2016. **2016**.
6. DONTREE S. Relation of Land Surface Temperature (LST) and Land Use/Land Cover (LULC) from Remotely Sensed Data in Chiang Mai – Lamphun Basin. SEAGA Conference 2010, Hanoi 2326 Nov 2010., 23. Retrieved from http://seaga.xtreemhost.com/seaga2010/CS5D_Dontree.pdf **2010**.
7. FU P., WENG Q. A time series analysis of urbanization induced land use and land cover change and its impact on land surface temperature with Landsat imagery. Remote Sensing of Environment, **175**, 205, **2016**.
8. SMITH A.M.S., KOLDEN C.A., TINKHAM W.T., TALHELM A.F., MARSHALL J.D., HUDAK A.T., GOSZ J.R. Remote sensing the vulnerability of vegetation in natural terrestrial ecosystems. Remote Sensing of Environment, **154**, 322, **2014**.
9. GUHA S., GOVIL H. An assessment on the relationship between land surface temperature and normalized difference vegetation index. Environment, Development and Sustainability, **23** (2), 1944, **2021**.
10. ZHOU X., WANG Y.C. Dynamics of Land Surface Temperature in Response to Land-Use/Cover Change. Geographical Research, **49** (1), 23, **2011**.
11. SIDDIQUI A., KUSHWAHA G., NIKAM B., SRIVASTAV S.K., SHELAR A., KUMAR P. Analysing the day/night seasonal and annual changes and trends in land surface temperature and surface urban heat island intensity (SUHII) for Indian cities. Sustainable Cities and Society, 75, **2021**.
12. PADDIES W.F. Estimating Soil Moisture with Landsat Data and Its Application in Extracting the Spatial Distribution of Winter Flooded Paddies. **2016**.
13. TRAN D.X., PLA F., LATORRE-CARMONA P., MYINT S.W., CAETANO M., KIEU H.V. Characterizing the relationship between land use land cover change and land surface temperature. ISPRS Journal of Photogrammetry and Remote Sensing, **124**, 119, **2017**.
14. JIANG J., TIAN G. Analysis of the impact of Land use/Land cover change on Land Surface Temperature with Remote Sensing. Procedia Environmental Sciences, **2** (5), 571, **2010**.
15. GEMITZI A., FALALAKIS G. Analyzing trends in Land Surface Temperature using remotely sensed time series data and the BFAST method, 6732, **2021**.
16. AKINYEMI F.O., IKANYENG M., MURO J. Land cover change effects on land surface temperature trends in an African urbanizing dryland region. City and Environment Interactions, **4** (2019), 100029, **2019**.
17. GARCÍA M.A., MOUTAHIR H., CASADY G.M., BAUTISTA S., RODRÍGUEZ F. Using hidden Markov models for land surface phenology: An evaluation across a range of land cover types in Southeast Spain. Remote Sensing, **11** (5), **2019**.
18. VERBESSELT J., HYNDMAN R., NEWNHAM G., CULVENOR D. Detecting trend and seasonal changes in satellite image time series. Remote Sensing of Environment, **114** (1), 106, **2010**.
19. AIGBOKHAN O.J. Forest Health Analysis, Using Remote Sensing and GIS Techniques: A Case Study of orest Health Analysis, Using Remote Sensing and GIS Techniques: A Case Study of Omo Forest Reserve, Ogun State. Nigeria. Continental J. Sustainable Development, **9** (2), 35, **2018**.
20. IBRAHIM G.R.F. Urban land use land cover changes and their effect on land surface temperature: Case study using Dohuk City in the Kurdistan Region of Iraq. Climate, **5** (1), **2017**.
21. ADEOLA FASHAE O., GBENGA ADAGBASA E., OLUDAPO OLUSOLA A., OLUSEYI OBATERU R. Land use/land cover change and land surface temperature of Ibadan and environs, Nigeria. Environmental Monitoring and Assessment, **192** (2), **2020**.
22. BHARATH SETTURU, RAJAN KS, R.T. Geostatistics: An Overview Land Surface Temperature Responses to Land Use Land Cover Dynamics. Geoinformatics & Geostatistics: An Overview, **1** (July), 1, **2013**.
23. WANG R., MURAYAMA Y. Geo-simulation of land use/cover scenarios and impacts on land surface temperature in Sapporo, Japan. Sustainable Cities and Society, **63**, 102432, **2020**.
24. NURLINA, KADIR S., KURNAIN A., ILHAM W., KALIMANTAN S., KALIMANTAN S., PROGRAM P.S. Comparison of Maximum Likelihood and Support Vector Machine Classifiers For Land Use/Land Cover Mapping Using Multitemporal Imagery, **12** (June), 126. Retrieved from http://www.savap.org.pk/journals/ARInt./Vol.12 (1)/ARInt.2021 (12.1-12).pdf **2021**.
25. ROTJANAKUSOL T., LAOSUWAN T. Model of relationships between land surface temperature and urban built-up areas in mueang buriram district, Thailand. Polish Journal of Environmental Studies, **29** (5), 3783, **2020**.
26. GUO J., WANG K., WANG T., BAI N., ZHANG H., CAO Y., LIU H. Spatiotemporal Variation of Vegetation NDVI and Its Climatic Driving Forces in Global Land Surface. Polish Journal of Environmental Studies, **31** (4), 3541, **2022**.
27. SABAJO C.R., LE MAIRE G., JUNE T., MEIJIDE A., ROUPSARD O., KNOHL A. Expansion of oil palm and other cash crops causes an increase of the land surface temperature in the Jambi province in Indonesia. Biogeosciences, **14** (20), 4619, **2017**.
28. RAMDANI F., MOFFIET T., HINO M. Local surface temperature change due to expansion of oil palm plantation in Indonesia. Climatic Change, **123** (2), 189, **2014**.
29. GOHAIN K.J., MOHAMMAD P., GOSWAMI A. Assessing the impact of land use land cover changes on land surface temperature over Pune city, India. Quaternary International, 575–576, 259, **2021**.
30. AIK D.H.J., ISMAIL M.H., MUHARAM F.M., ALIAS M.A. Evaluating the impacts of land use/land cover changes across topography against land surface temperature in Cameron Highlands. PLoS ONE, **16** (5 May), 1, **2021**.
31. VERHOEVEN J.T.A., SETTER T.L. Agricultural use of wetlands: Opportunities and limitations. Annals of Botany, **105** (1), 155, **2010**.
32. GAROUANI, M. EL, AMYAY M., LAHRACH A., OULIDI H.J. Land Surface Temperature in Response to Land Use/Cover Change Based on Remote Sensing Data and GIS Techniques: Application to Saïss Plain, Morocco. Journal of Ecological Engineering, **22** (7), 100, **2021**.
33. LAOSUWAN T., GOMASATHIT T., ROTJANAKUSOL T. Application of remote sensing for temperature monitoring: The technique for land surface temperature analysis. Journal of Ecological Engineering, **18** (3), 53, **2017**.
34. NURLINA, RIDWAN I., HADI HARYANTI N., HANIK U. Analysis of Environmental Vulnerability Using Satellite Imagery and Geographic Information System in Coal Mining Area Planning at Banjar Regency. IOP Conference Series: Earth and Environmental Science, **499** (1). **2020**.

35. KADIR S., BADARUDDIN, NURLINA, FARMA E. Power Recovery Support Tabunio Watershed Based on Analysis of Erosion Based on Geographic Information System in the Province of South Kalimantan. Mediterranean Journal of Social Sciences, **8** (4-1), 73, **2017**.
36. AULIANA A., RIDWAN I., NURLINA N. Analisis Tingkat Kekritisan Lahan di DAS Tabunio Kabupaten Tanah Laut. POSITRON, **7** (2), 54, **2018**.
37. KADIR S., BADARUDDIN, NURLINA, RIDWAN I., RIANAWATY F. The recovery of Tabunio watershed through enrichment planting using ecologically and economically valuable species in south Kalimantan, Indonesia. Biodiversitas, **17** (1), 140, **2016**.
38. SAPUTRA A.E., RIDWAN I., NURLINA N. Analisis Tingkat Resapan Air Menggunakan Sistem Informasi Geografis di Das Tabunio, **1**, 149, **2019**.